Hexagonal or trigonal structure of ettringite revisited by Raman spectroscopy

G. Renaudin, R. Segni, F. Leroux, C. Taviot-Gueho
Université Blaise Pascal, Clermont-Ferrand, France.
Corresponding author: guillaume.renaudin@ensccf.fr

Abstract
Crystal structure of ettringite, $Ca_6Al_2(OH)_{12}\cdot(SO_4)_3\cdot 26H_2O$, is up to now not definitive as one hexagonal $P\bar{6}2c$ model was proposed by Courtois et al. in 1968 and one trigonal $P31c$ model was proposed by Moore and Taylor in 1968 and improved in 1970. Moore and Taylor attributed the hexagonal description of ettringite to twinning. Main difference between the two models is the number of sulphate anions independent crystallographic sites: two independent SO_4^{2-} tetrahedra with statistical occupational disorder in the hexagonal description or a fully ordered trigonal description with three SO_4^{2-} tetrahedra with the same multiplicities. Distinguish between the two models by X-ray diffraction is quite impossible without ambiguity. Then, the aim of this work was to use Raman spectroscopy as a probe of local environment and point symmetry of sulphate groups. Present ettringite powder sample was synthesized by a coprecipitation method. Profile fitting on Raman spectrum of the symmetric stretching ν_1 SO_4^{2-} mode corresponds to the ordered structure in the trigonal $P31c$ space group. The hydrogen bonds network was also identified by profile fitting of the OH^- and H_2O stretching massifs combined to the use of the Falk law. During the preparation time of this manuscript, a neutron powder diffraction investigation on deuterated ettringite has been published by Hartman and Berliner. Their Rietveld refinement led to the definitive fully ordered trigonal $P31c$ description of ettringite structure in perfect agreement with our spectroscopic present results.

1. Introduction

Ettringite, a hydrated basic sulphate of aluminium and calcium with chemical composition $Ca_6Al_2(OH)_{12}\cdot(SO_4)_3\cdot 26H_2O$, occurs as a natural mineral, and is technically important as a hydration product of Portland cement. It forms hexagonal prismatic crystals which are often highly elongated in cement paste. The crystal structure of ettringite has been investigated for many years. The first single crystal X-ray study was made by Bannister et al. in 1936 [2]. They obtained a hexagonal unit cell with a = 11.26 Å and c = 21.48 Å (Z = 2) and proposed the $P6_3/mmc$ space group. Evidences for crystallographic analogies have been observed with

thaumasite $Ca_6Si_2(OH)_{12}\cdot(SO_4)_2\cdot(CO_3)_2\cdot 24H_2O$ [3] and jouravskite $Ca_6Mn_2(OH)_{12}\cdot(SO_4)_2\cdot(CO_3)_2\cdot 24H_2O$ [4], having both the $P6_3$ symmetry. This suggested the structure was based on chains of Ca^{2+} and $Al(OH)_6^{3-}$ ions, between which were SO_4^{2-} anions and H_2O molecules. Two structural works were published for ettringite almost simultaneously and independently in 1968. Courtois et al. proposed a hexagonal $P\bar{6}2c$ model [5], while Moore and Taylor indicated a trigonal $P31c$ model [6]. These two proposed space groups gave substantially similar description of the structure, which confirmed the general prediction from the first single crystal study [2]. The trigonal $P31c$ model is fully ordered with 26 independent atomic positions: two crystallographic sites for aluminium, two for calcium and three for sulphur atoms. In this description the 6 sulphate anions per unit cell are fully ordered with the point symmetry 3, S atoms occupying three independent $2b$ (⅓,⅔,z) sites. The hexagonal $P\bar{6}2c$ model has 16 independent atomic positions: one crystallographic site for aluminium, two for calcium and two for sulphur atoms. The 6 sulphate anions with also the point symmetry 3 are described with S on two independent $4f$ (⅓,⅔,z) sites. One of these two SO_4 tetrahedra is half occupied, this model presenting a statistical disorder. Moore and Taylor attributed the hexagonal description of ettringite to twinning. The structure description is up to now not definitive as differences between the two models are weak: the number of independent atomic position and the point symmetry of calcium atoms (2 and *m* in hexagonal model, and 1 in trigonal model). Differentiate both models by X-ray diffraction is thus quite impossible and owing to the close resemblance in the diffracted rotation photographs with thaumasite, Moore and Taylor indicate a description of an average-structure in a halved unit cell volume (halved value of *c* axis) with the hexagonal $P6_3/mcm$ space group. In this average substructure model all the sulphates anions are described by unique SO_4 tetrahedra. S atoms are on site $4d$ (⅓,⅔,0) with a site symmetry 3·2. Sulphate anions show a statistical occupational disorder (partial occupancy for the atomic sites describing sulphate) and an orientation disorder due to the presence of the mirror normal to *c* axis. Then, the aim of the present work is to use Raman spectroscopy as a probe of local environment and point symmetry of sulphate groups. The hydrogen bond network, allowing the connection of main columns of hydrated calcium and aluminium hydroxyls with intercolumnar sulphate anions and water molecules, was also identified by profile fitting of the Raman OH^- and H_2O stretching massifs combined to the use of the Falk law [7]. During the preparation time of this manuscript, a neutron powder diffraction investigation on deuterated ettringite has been performed by Hartman and Berliner [1]. In perfect agreement with our present spectroscopic results, their crystallographic study led to the definitive trigonal $P31c$ description of ettringite. Atomic positions of Ca, Al, S and O atoms from Moore and Taylor data [6] were confirmed and hydrogen (deuterium) sites were localized [1].

2. Experimental

2.1 Samples synthesis and materials

Ettringite phase was prepared within two days by the coprecipitation method [8]. To the best of our knowledge, there is no report in the literature of such preparative procedure for ettringite. The synthesis was performed at room temperature at controlled pH, using demonized and decarbonated water and under nitrogen atmosphere in order to avoid contamination by carbonate anions. 20 mL of a mixed solution of $CaCl_2$ 0.66M and $AlCl_3$ 0.33M were added dropwise to a reactor, containing 250 mL Na_2SO_4 0.08 M representing an excess of 6 equivalents of sulfate anions over Al^{3+} content used ; the pH was kept constant at 11.5 $\pm$ 0.1 by the simultaneous addition of 2.0 M NaOH solution. Before starting the addition, a few drops of H_2SO_4 1M were added to the reaction mixture up to a pH value of 4 as an additional source of sulfate anions. After complete addition of the metallic salts, the precipitate was aged in the mother solution for 48 hours at the same temperature as the synthesis i.e. room temperature. The good cristallinity of the final product allowed us to perform a refinement of the cell parameters in the space group *P*31*c* using the Profil Matching option of *FullProf* program [9]: *a* = 11.2349 (2) Å and *c* = 21.44662 (6) Å.

Two commercial products had been used to validate the profile fitting procedure on Raman spectra: gypsum ($CaSO_4 \cdot 2H_2O$, Merk, for analysis, purity > 99%) and thenardite (Na_2SO_4, Prolabo, normapur, purity > 99.9%). These two sulphate containing products were chosen because of their crystallographic structures and sulphate local environments are well known. Both structures contain unique sulphate independent anion.

2.2 Raman spectroscopy

Micro-Raman spectra were recorded at room temperature in the back scattering geometry, using a Jobin-Yvon T64000 device in a single mode with 1800 grooves per mm grating. The spectral resolution obtained with an excitation source at 514.5 nm (argon ion laser line, Spectra Physics 2017) is about 2 cm^{-1}. The Raman detector is a charge coupled device (CCD) multichannel detector cooled by liquid nitrogen to 140 K. The laser beam was focused onto the sample through an Olympus confocal microscope with x100 magnification. Laser spot was about 1 μm^2. Measured power at the sample level was kept low (less than 15 mW) in order to avoid any damage to the material. The Raman scattered light was collected with the microscope objective at 180 ° from the excitation and filtered with an holographic Notch filter before being dispersed. Spectra were recorded at room temperature and were analyzed by using the profile fitting procedure with a Voigt function (Lorentzian and Gaussian combination) of the program *SPECTRAW* [10].

3. Results

Raman spectra were measured with a high counting rate allowing good profile fitting. Spectra were recorded in the range 225 cm^{-1} to 1275 cm^{-1} to visualize the four Raman active vibration modes of sulphate anions, as well as in the range from 2800 cm^{-1} to 4000 cm^{-1} to investigate the hydrogen bond network due to the hydroxyl and water stretching mode. Figure 1 shows the recorded spectra with assignments.

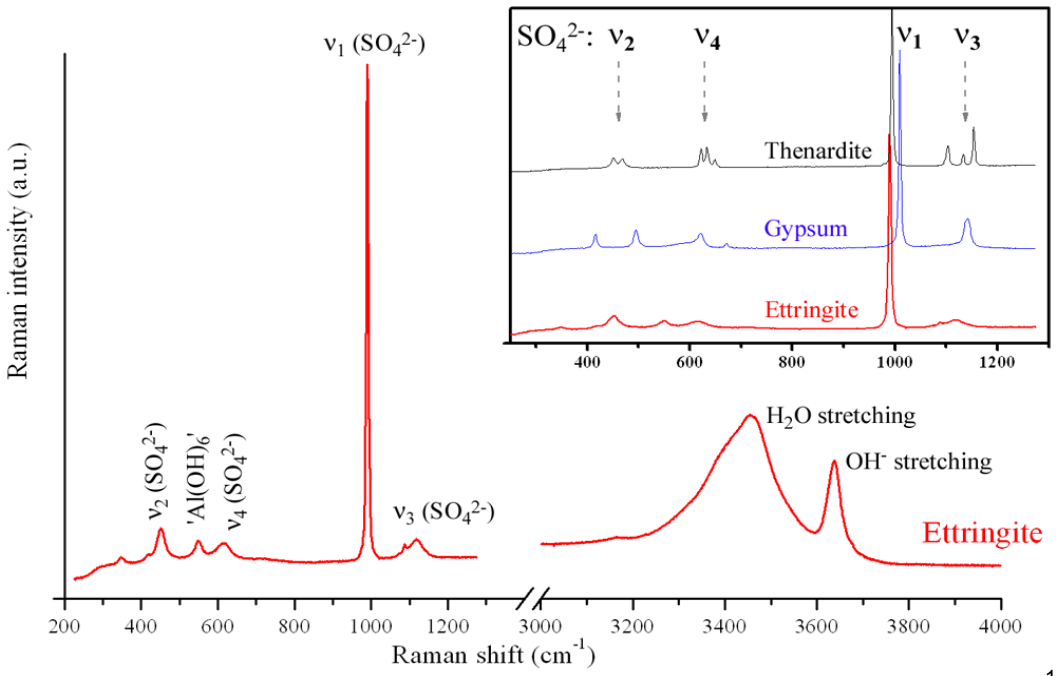

Figure 1. Main window: Raman spectra of ettringite in the ranges 225 cm^{-1} – 1275 cm^{-1} and 3000 cm^{-1} – 4000 cm^{-1} recorded at room temperature. Inset window (top right): Raman sulphate modes of vibration in ettringite (red), gypsum (blue) and thenardite (black).

3.1 point symmetry of sulphate anions

The point symmetry of sulphate anion was used to investigate the space group of ettringite. Table 1 gives the correlation diagrams for internal vibrations of tetrahedral SO_4^{3-} anions in the proposed hexagonal $P\bar{6}2c$ and $P31c$ descriptions. The correlation diagram corresponding to the hexagonal $P6_3/mcm$ average model is also indicated, as well as the two reference materials (gypsum and thenardite) used to validate the method.

Table 1. Correlation diagrams for internal vibrations of tetrahedral SO_4^{3-} groups in the different structural models for ettringite, and in the two reference materials (gypsum and thenardite):

Fundamental modes	Site symmetry					
	Free ion	Ettringite			Gypsum	Thenardite
		*P*6$_3$/*mcm* $\rightarrow D_{6h}^3$	*P*$\bar{6}$2*c* $\rightarrow D_{3h}^4$	*P*31*c* $\rightarrow C_{3v}^2$	*C*2/*c* $\rightarrow C_{2h}^6$	*Fddd* $\rightarrow D_{2h}^{24}$
	T_d	C_3 (*) 1 site	C_3 2 sites	C_3 3 sites	C_2 1 site	D_2 1 site
ν_1	A_1	A	A	A	A	A
ν_2	E	E	E	E	2A	2A
ν_3	T_2	A+E	A+E	A+E	A+2B	$A_1+A_2+A_3$
ν_4	T_2	A+E	A+E	A+E	A+2B	$A_1+A_2+A_3$

(*) site symmetry D_3' with an orientation disorder due to the mirror normal to *c* axis lead to an effective site symmetry C_3 for the sulphate tetrahedron.

The three proposed models for ettringite give the same irreducible representation of the internal SO_4^{3-} vibrations. In all cases, the point symmetry of SO_4^{3-} is C_3. This is evident in the *P*$\bar{6}$2*c* (D_{3h}^4) and *P*31*c* (C_{3v}^2) cases. In the case of the *P*6$_3$/*mcm* (D_{6h}^3) average model, the apparent D_3' point symmetry becomes C_3 when removing the mirror plane normal to *c* axis. The incompatible D_3' point symmetry for the tetrahedral sulphate ion is due to its orientation disorder. In the case of C_3 point symmetry, the symmetric and asymmetric bending ν_3 and ν_4 modes show a splitting of the degeneracy in two components ν_3, ν_3' and ν_4, ν_4' respectively. Both ν_3 and ν_4 splitting are not resolved on the Raman spectra, particularly in the case of ν_4 and ν_4' bands. Probably the large band broadening masks the splitting of two components. In gypsum, the point symmetry of sulphate is C_2, leading to the following splitting of the degenerate vibrations: asymmetric stretching ν_2 mode splits in two ν_2 and ν_2' components, ν_3 (and ν_4) mode splits in three ν_3, ν_3' and ν_3'' (and ν_4, ν_4' and ν_4'') components. Sulphate anion in thenardite, with the point symmetry D_2, follows the same irreducible representation of the internal modes as gypsum (see Table 1). As indicated by the inset of Figure 1, modes splitting are perfectly resolved in case of thenardite: one band for symmetric stretching ν_1 mode, two bands for ν_2 mode, three bands for ν_3 and ν_4 modes. For the three compounds the ν_1 mode is by far the best resolved and corresponds to the more intense vibration band. Then the ν_1 band was used for the profile fitting procedure. The aim of the fitting is to find the number of components in this ν_1 band in case of ettringite spectra. The number of component should indicate the number of crystallographic independent sites in the structure: one for the *P*6$_3$/*mcm* average model, two for the *P*$\bar{6}$2*c* hexagonal model and three for the *P*31*c* trigonal model. Furthermore, the intensity ratio (i.e. surface ratio) between the different components has to be respected. The *P*$\bar{6}$2*c* hexagonal description leads

to the 2/1 (because site occupancies of the two independent sulphates are 1 and ½). The sites of the three independent sulphate anions in the *P*31*c* trigonal description are fully occupied, so the 1/1/1 ratio is expected. In order to validate the method, the band corresponding to the ν_1 mode in gypsum and thernardite should be perfectly reproduced by using a unique component (sulphate anions occupy a unique site in both structures [11, 12]). Figure 2 shows the good profile fitting obtained for gypsum and thernardite using one component.

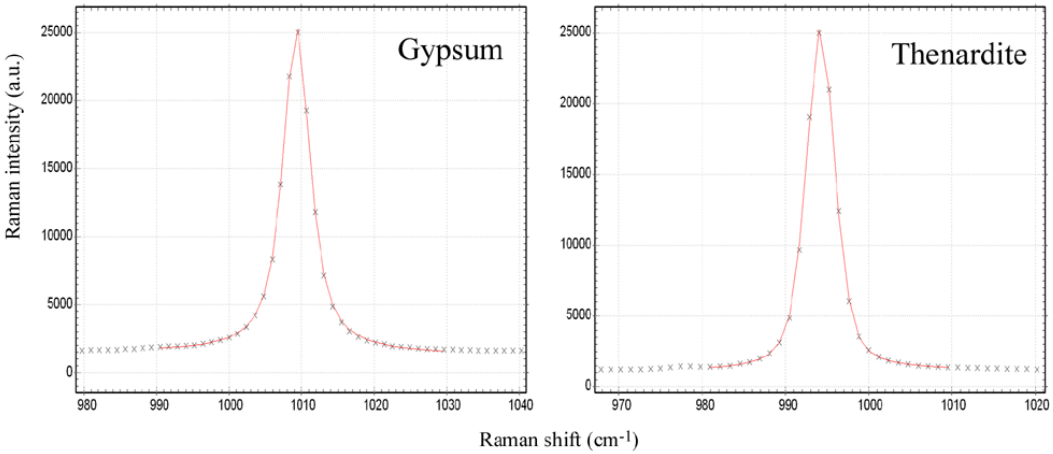

Figure 2. Profile fitting (curve) of ν_1 mode in measured Raman spectra (cross) with one component for gypsum (left) and thenardite (right).

Figure 3 and Table 2 display the results of the profile fitting procedure on SO_4^{2-} ν_1 band in ettringite. Clearly, the use of a unique component corresponding to the *P*6$_3$/*mcm* average model led to a bad fitting due to an evident asymmetrical shape of the band. The Half Width at Half Maximum (HWHM) of the band in ettringite is broad compared to gypsum and thenardite (3.06 cm^{-1} compared to respectively 2.27 and 2.06 cm^{-1}). Although the asymmetrical shape of the ν_1 band was not perfectly fitted by using two components, the fitting is quite acceptable. However, as indicated in table 2, the fitted surface area ratio of 1/1.25 between the two components disagrees with the expected 1/2 ratio for the $P\bar{6}2c$ hexagonal model. On the other hand, the band decomposition performed with three components indicates a perfect fitting and the fitted surface area ratio 1/1.07/1.16 is close to the expected 1/1/1 in the case of the *P*31*c* trigonal model. This profile fitting procedure is in favour of *P*31*c* trigonal description. Recent works of Hartmann and Berliner [1] led to the same conclusion. Indeed, the authors made a powder neutron diffraction pattern Rietveld refinement of deuterated ettringite in the *P*31*c* description allowing the localisation of hydrogen (deuterium) positions. Of course, the neutron structural study of Hartmann and Berliner is a more definitive indication for the symmetry of ettringite; the comparison of the data brings a good validation of our spectroscopic study. The close features of the

three components of the ν_1 band, i.e. Raman shift and HWHM mentioned in Table 2, is also in perfect agreement with Hartman's results [1]. The three independent sulphate groups have exactly the same environment. Only weak differences appear in the interatomic distances. Each sulphate anion is neighboured by twelve hydrogen atoms (at a distance from sulphur central atom between 2.72 Å and 3.27 Å). These twelve hydrogen atoms belong to twelve water molecules linked to calcium cations (with oxygen atoms at a distance to sulphur central atom between 3.53 Å and 3.88 Å).

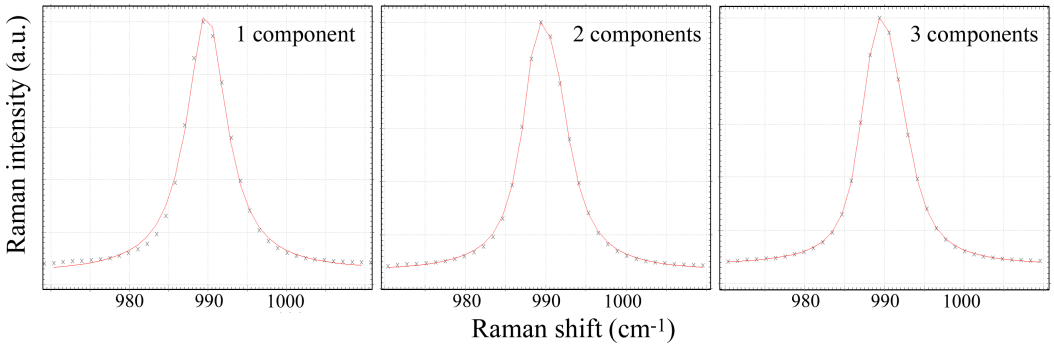

Figure 3. Profile fitting (red curve) of sulphate ν_1 mode from ettringite Raman spectra (cross) with one (left), two (middle) and three (right) components.

Table 2. Profile fitting results of sulphate ν_1 mode from Raman spectra.

Sample	number of components	Raman shift (cm^{-1})	HWHM (*) (cm^{-1})	Surface area (a.u.)	Surface ratio
Gypsum	1	1009.3	2.27	$1.56\ 10^5$	-
Thenardite	1	994.2	2.06	$1.28\ 10^5$	-
Ettringite	1	989.8	3.06	$2.37\ 10^5$	-
	2	988.7 991.0	2.14 2.70	$0.96\ 10^5$ $1.21\ 10^5$	1/1.25
	3	988.0 989.8 991.8	1.90 1.73 2.37	$0.61\ 10^5$ $0.65\ 10^5$ $0.71\ 10^5$	1/1.07/1.16

(*) Half Width at Half Maximum.

3.2 Hydrogen bonds network

Micro-Raman spectra recorded in the range 3000 cm^{-1} – 4000 cm^{-1} allowed us to investigate the hydrogen bonds network. Figure 4 shows the fit performed in this range. Spectra is mainly composed of a broad band with maximum at 3455 cm^{-1} and HWHM of 86 cm^{-1} attributed to the stretching vibration of water molecules and a sharp signal centered at 3638 cm^{-1} and HWHM of 14 cm^{-1} attributed to the stretching of hydroxyl. A

third weak band is observed at 3165 cm^{-1} with HWHM of 15 cm^{-1}. Two shoulders on the broad vibration band of water molecules are also observed at 3300 cm^{-1} and 3400 cm^{-1}. The empirical Falk law [7] can be used to deduce the length of the hydrogen bond (interatomic distance between donor oxygen atom to acceptor oxygen atom of the hydrogen bond) from the position of its corresponding stretching vibration. In the following Falk law, ν is the position (in cm^{-1}) of the stretching band and r is the hydrogen bond length (in Å):

$$\nu = 3707 - \frac{3707}{2727} \exp(20.96 - 5.539\ r)$$

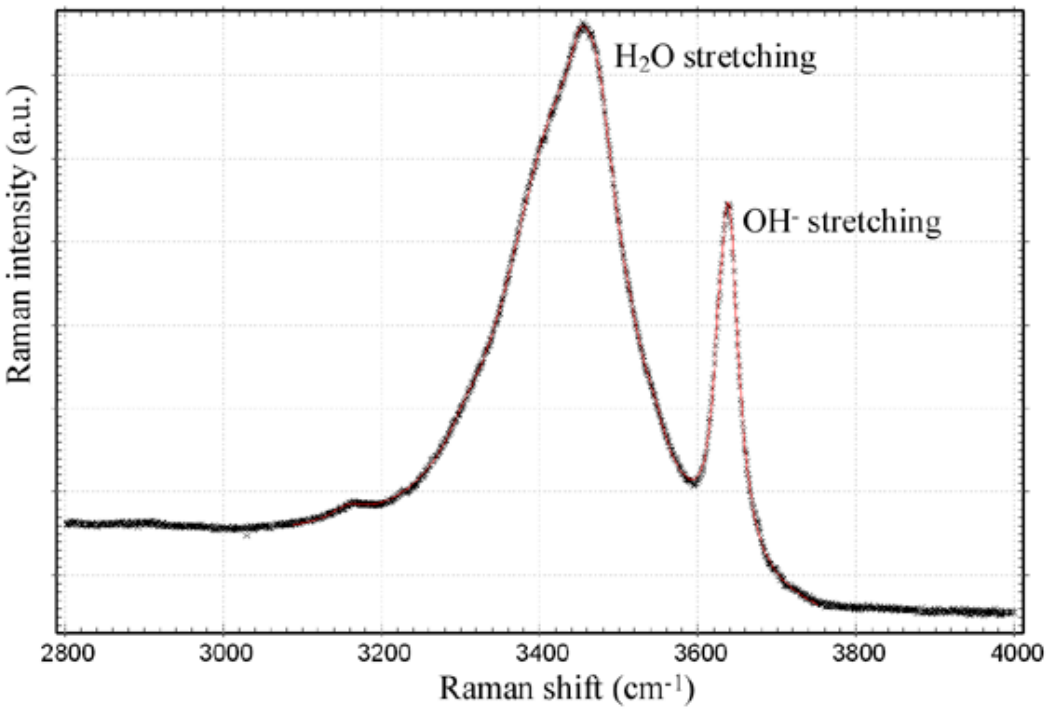

Figure 4. Profile fitting (red curve) of the measured Raman spectra (cross) in the range 3000 cm^{-1} - 3800 cm^{-1} corresponding to the stretching of the hydrogen bonds network in ettringite.

The hydroxyl band centered at 3638 cm^{-1} was decomposed in ba nds ranging from 3626 cm^{-1} to 3652 cm^{-1}, corresponding to a hydrogen bond lengths from 3.05 Å to 3.12 Å. The broad band can be decomposed in several bands ranging from 3303 cm^{-1} to 3544 cm^{-1} that correspond to hydrogen bond lengths, from 2.76 Å to 2.92 Å; the weak band at 3165 cm^{-1} involves a hydrogen bond length of 2.70 Å. Applying a standard deviation of more or less 0.1 Å to these empirically calculated interatomic distances, we can assume that hydrogen bonds involved by hydroxyl anions and by water molecules, have to be attributed for oxygen-oxygen distances 2.95 Å < $d_{OH^- - O}$ < 3.22 Å, and 2.60 Å < $d_{H_2O - O}$ < 3.02 Å

respectively. To be considered as a possible acceptor, the neighboring oxygen atom cannot participate to the same coordination polyhedra as the donor. These informations are gathered in Table 3 together with inter-oxygen distances according to [6] and [1]. This Raman study on water and hydroxyl stretching vibrations clearly demonstrates the possibility to identify and localize hydrogen bonds in the structure even if hydrogen positions are missed. The hydrogen bond network deduced from our spectroscopic study is exactly the same that has been solved by Hartman and Berliner [1]. The only missing hydrogen bond in our study is O12-H12a---O10 expected at 3.12 Å and excluded from our 2.60 Å < d_{H_2O-O} < 3.02 Å range because of its weakness. A discrepancy can also be observed on the O19 free water case which can be easily attributed to its half site occupancy. Indeed, refined interatomic distances can be artificially decreased as a result of statistical disorder. In this way the indicated O19-H19b---O19 hydrogen bond with $d_{O19-O19}$ = 2.37 Å appears very short (with a corresponding stretching band around 2940 cm^{-1}). In spite of this uncertainty, we found the general feature of the hydrogen bond network in ettringite. Hydroxyl groups involve intra-column hydrogen bonds along the $[Ca_3Al(OH)_6(H_2O)_{12}]^{3+}$ columns. Linked water molecules involve two kinds of hydrogen bonds: a small part, i.e. one eighth, is intra-column perpendicular to the column; the others seven eighth give the inter-column cohesion through of sulphate anions and free water molecules.

Table 3. Hydrogen bonds interpretation to the profile fitting results of the Raman spectra in the range 3000 cm^{-1} - 3800 cm^{-1} in ettringite.

Donor O-H [(a)]	O Neighbour [(b)]	Possible acceptor H---O [(c)]	Hydrogen bond length O-H---O [6] (Å)	[1] (Å)	Hydrogen bonds from [1]
Hydroxyls:					
O1	O3	-	3.07	2.98	
	O12	-	3.08	3.06	
	O10	-	3.11	3.09	
	O5	Yes	3.19	3.27	O1-H1---O5
O2	O9	-	2.94	3.04	
	O4	-	3.03	3.02	
	O11	-	3.07	3.27	
	O6	Yes	3.17	3.06	O2-H2---O6
	O5	-	3.39	3.21	
O3	O12	-	2.94	2.96	
	O10	-	2.95	3.04	
	O1	-	3.07	3.07	
	O7	Yes	3.22	3.25	O3-H3---O7
O4	O2	-	3.03	3.04	
	O8	Yes	3.12	3.10	O4-H4---O8

	O11	-	3.12	2.93	
	O9	-	3.24	3.00	
Linked water:					
O5	O18	Yes	2.82	2.79	O5-H5a---O18
	O16	Yes	2.98	2.85	O5-H5b---O16
O6	O18	Yes	2.65	2.70	O6-H6b---O18
	O16	Yes	2.70	2.70	O6-H6a---O16
	O10	-	3.08	2.99	
O7	O17	Yes	2.77	2.95	O7-H7b---O17
	O19	Yes	3.06	2.88	O7-H7a---O19
	O11	-	3.10	2.92	
O8	O19	Yes	2.50	2.64	O8-H8a---O19
	O17	Yes	2.83	2.80	O8-H8b---O17
	O12	-	2.91	2.95	
O9	O16	Yes	2.60	2.81	O9-H9b---O16
	O17	Yes	2.82	2.55	O9-H9a---O17
	O11	Yes	2.82	2.85	O11-H11a---O9
	O2	-	2.94	3.02	
	O4	-	3.24	3.00	
O10	O14	Yes	2.90	2.87	O10-H10a---O14
	O18	Yes	2.95	2.87	O10-H10b---O18
	O3	-	2.95	3.07	
	O6	-	3.08	2.99	
O11	O9	Yes	2.82	2.85	O11-H11a---O9
	O15	Yes	2.88	2.90	O11-H11b---O15
	O19	Yes	2.94	2.69	O19-H19b---O11
	O7	-	3.10	2.92	
	O4	-	3.12	2.93	
O12	O13	Yes	2.82	2.76	O12-H12b---O13
	O8	-	2.91	2.95	
	O3	-	2.94	3.04	
Free water:					
O19	O19	Yes	2.42	2.37	O19-H19b---O19
	O8	Yes	2.50	2.64	
	O11	Yes	2.94	2.69	O19-H19b---O11
	O7	Yes	3.06	2.88	

[(a)] Atom labels are those from [6] and [1], [(b)] Considered neighbour oxygen atoms are those involving an interatomic distance in relation with Falk law calculation (i.e. 2.60 Å < $d_{Donor\text{-}Acceptor}$ < 3.05 Å for hydrogen bond from water molecule, and 2.95 Å < $d_{Donor\text{-}Acceptor}$ < 3.22 Å for hydrogen bond from hydroxyl), [(c)] Neighbour oxygen atom is considered as possible acceptor only if it does not belong to the same coordination sphere as the donor.

4. Conclusion

The point symmetry of sulphate anions and the number of independent sulphate anions have been used to interpret micro-Raman spectrum of ettringite in order to determine its space group. The profile fitting of the symmetric stretching ν_1 mode of tetrahedral SO_4^{2-} anions has allowed us to attribute the trigonal *P*31*c* space group to ettringite in agreement with data from [6] and recently confirmed by [1]. In the same way, hydrogen bond network has been characterized by profile fitting of the H_2O and OH^- stretching bands combined with structural data in which hydrogen sites are missed (i.e. structural data obtained from X-rays diffraction). This study gives a good example of the ability of micro-Raman spectroscopy to bring important additional details to complete a structural characterization as mentioned in [13], namely in case of hydrated anionic compounds as encountered in cement chemistry.

Acknowledgement
The authors are grateful to J.-M. Nedelec from University Blaise Pascal for his help with the micro-Raman apparatus.

References

[1] M.R. Hartman, R. Berliner, Investigation of the structure of ettringite by time-of-flight neutron powder diffraction technique, Cem. Concr. Res. 36 (2006) 364-370.
[2] F.A. Bannister, M.H. Hey, J.D. Bernal, Ettringite from Scawt Hill, Miner. Mag. 24 (1936) 324-328.
[3] E. Welin, The crystal structure of thaumasite $Ca_3H_2(CO_3SO_4)SiO_4(H_2O)_{13}$, Ark. Min. Geol. 2 (1957) 137-147. See also S.D. Jacobsen, J.R. Smith, R.J. Swope, Thermal expansion of hydrated six-coordinate silicon in thaumasite, $Ca_3Si(OH)_6(CO_3)(SO_4)\cdot 12H_2O$, Phys. Chem. Min. 30 (2003) 321-329.
[4] M.M. Granger, J. Protas, Détermination et étude de la structure crystalline de la jouravskite $Ca_3Mn(SO_4)(CO_3)(OH)_6(H_2O)_{12}$, C. R. Acad. Sci. Paris Série D 262 (1966) 1037-1039. See also M.M. Granger, J. Protas, Determination et etude de la structure crystalline de la jouravskite $Ca_3Mn^{IV}(SO_4)(CO_3)(OH)_6\cdot 12(H_2O)$, Acta Cryst. B 25 (1969) 1943-1951.
[5] A. Courtois, Y. Dusausoy, A. Lafaille, J. Protas, Etude préliminaire de la structure cristalline de l'ettringite, C. R. Acad. Sci. Paris Série D 266 (1968) 19111913.
[6] A.E. Moore, H.F.W. Taylor, Crystal structure of ettringite, Nature 218 (1968) 1048-1049. See also A.E. Moore, H.F.W. Taylor, Acta Cryst. B 26 (1970) 386-393.
[7] M. Falk, Chemistry and physics of aqueous gas solution, Adam W.A. Edition, Princeton, 1975.
[8] S. Miyata, Clays Clay Min., 31 (1983) 305-311.

[9] J. Rodriguez-Carvajal, PROGRA*M* *FullProf.2k* – version 3.30, Laboratoire Léon Brillouin (CEA-CNRS), France, 2005.
[10] D. Lovy, Program *SPECTRAW*, Version 1.40, Dept. de Chimie Physique, University of Geneva, 1996.
[11] J.C.A Boeyens, V.V.H. Ichharam, Redetermination of the crystal structure of calcium sulphate dehydrate $CaSO_4 \cdot 2H_2O$, Zeit. Krist. 217 (2002) 9-10.
[12] S.E. Rasmussen, J.-E. Jorgensen, B. Lundtoft, Structure and phase transition of Na_2SO_4, J. Appl. Cryst. 29 (1996) 42-47.
[13] S.S. Potgieter-Vermaak, J.H. Potgieter, R. Van Grieken, The application of Raman spectroscopy to investigate and characterize cement, Part I: A review, Cem. Concr. Res. 36 (2006) 656-662.